X-Ray microscopy imaging of reactive transport and drying of salt solutions in fractured porous media from core- to pore- scale

I. Daher†, J.P. Crawshaw†, G.C. Maitland† and E.S. Boek†

† Qatar Carbonates and Carbon Storage Research Centre (QCCSRC),
Department of Chemical Engineering, Imperial College London, London SW7 2AZ

This paper was prepared for presentation at the International Symposium of the Society of Core Analysts held in Avignon, France, 8-11 September, 2014

ABSTRACT

During the sequestration of CO_2 into down-hole rock formations, salt precipitation may occur due to drying of the brine associated with the CO_2 injection process. Previous work [1, 2] showed that the location of the precipitate depends on the competition of advective and capillary forces on the aqueous fluid phase transporting brine to the drying front. Here we consider the drying process of reservoir brine in fractured porous media by the injection of sub-saturated CO_2. In the case of a heavily fractured reservoir, the injected CO_2 will start drying the fracture-matrix interface, which may result in capillary driven transport of brine and salt to the fracture-matrix interface, where it potentially will precipitate. The morphology and the exact location of the precipitate at the interface are the crucial issues to solve. In certain circumstances, the precipitate forms a low permeability layer in the fracture space, reducing the fracture permeability (injectivity) leading to an increase of the injection pressure. Precipitation in fractures is a multi-scale problem which requires imaging on different length scales: the propagation of the dry zone and the location of the precipitate on the fracture or core scale, and the location of precipitation at the fracture-matrix interface on the pore scale.

INTRODUCTION

The CO_2 injected into the formation is usually dry and therefore the formation water will evaporate into the CO_2 phase. This can happen near the wellbore or more extensively in a fractured reservoir where the fractures will be rapidly filled with the dry CO_2. The precipitation of salt and its scaling around wellbore depends on the mobility of the brine. Salt precipitated during drying can lead to reductions in porosity and permeability of the reservoir in the vicinity of the wellbore [3].

In porous media exposed at one face to under saturated vapour or capillary tubes open at one end, there are two main stages of evaporation. Typically, there is an early stage of evaporation with a relatively high and constant evaporation rate, known as stage-1 evaporation or the Constant Rate Period (CRP), followed by a much lower evaporation rate known as stage-2 evaporation or the Falling Rate Period (FRP) [4]. Stage-1 is associated with a liquid film connection to the exposed surface, see figure 1. Chauvet [5] mentioned a third stage which is Receding Front Period (RFP), this is however a split of the second stage into two (i.e. first falling rate period, FRP1 and second falling rate period, FRP2, Scherer [6] called this receding front period, RFP as Falling rate period 2, FRP2).

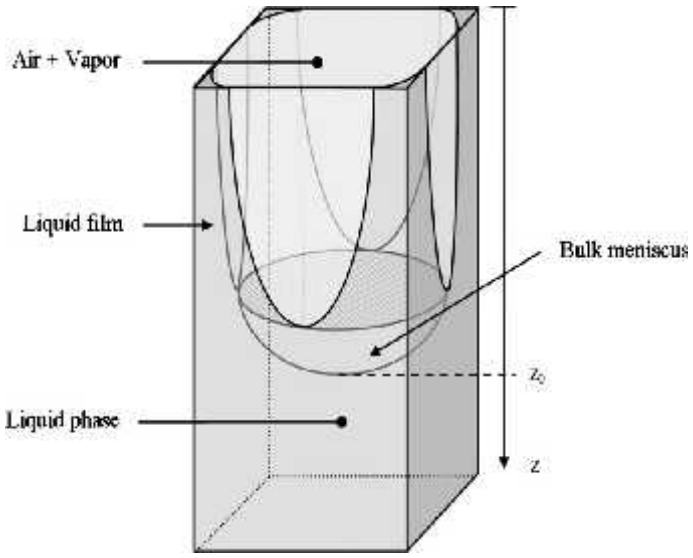

Figure 1 Sketch of the thick liquid films in a capillary tube of square cross section. (The bulk meniscus position is denoted as z_o.) [7]

Here we investigate the effect of injecting CO_2 into a fractured rock and study the mass transfer between matrix and fracture orthogonal to the flow direction in the fracture by considering the analogous system of a core exposed at one face to dry air. This was done by a combination of experiments and modelling. The experimental methods employed were mass loss measurements with carefully controlled boundary conditions and micro-CT imaging of the location of salt deposits.

EXPERIMENTAL METHOD

Cores and solutions: We use two different types of rocks in our study. Bentheimer sandstone has an intergranular pore space. Ketton limestone is an oolitic quarry limestone of Jurassic age. The grains are mostly smooth micro-porous spheres. The micro-pores were not resolved by the micro-CT imaging used. Solutions used in the experiment are de-ionized water or saturated sodium chloride solution.

Single phase permeability measurement: The main purpose of the core flooding experiment is to obtain initial porosity and permeability. A core holder was made to accommodate the samples. First, they are flooded with CO_2 followed by the required liquid phase that dissolves the residual CO_2 to achieve 100 % liquid saturation in the sample prior to dry-out experiment. All our samples of an appropriate size for Micro-CT imaging; 2 or 4.5 cm in length and 6 mm in diameter.

Dry-out experiment: As soon as the core-flooding experiment is finished, samples are put in an oven sealed inside an impermeable layer. Once the sample has reached the oven temperature one end of the core is exposed and a micro-fan is used to allow continuous air flow over the exposed face. Desiccants are used inside the oven to ensure zero humidity and the mass loss is recorded by continuous data logging.

Imaging: An Xradia XRM 500 Micro-CT was used to take images of the samples and the salt deposits. The X-ray source was operated at 80 kV voltage, 7W power and 80 μA current. A 4X magnification was used to achieve the voxel size resolution of $2.5x2.5x2.5\mu m^3$ across 6 mm of a

cylindrical core sample.

RESULTS AND DISCUSSION

Our initial experiments started with de-ionised (DI) water in 2cm long Bentheimer cores at 30°C and 60°C degrees. As is shown in Figure 2, a constant high evaporation rate persists until the liquid phase saturation drops below around 0.2. As explained in the introduction this regime is expected to exist as long as there is a capillary driven flow that supports the connection through the liquid phase between the drying front and the matrix surface. Below a saturation of 0.2 the evaporation slows and becomes non-linear in time. It is not clear from this data if this is when the capillary connection breaks or if this is an end effect. The difference in the slope of the linear part of the drying curve, drying is 3.5 times faster at 60°C can mostly be explained by the difference in the vapour pressure of water between the two temperatures; 4247 Pa and 19950 Pa at 30°C and 60°C respectively. Figure 2 also shows the excellent reproducibility of the water dry-out experiments.

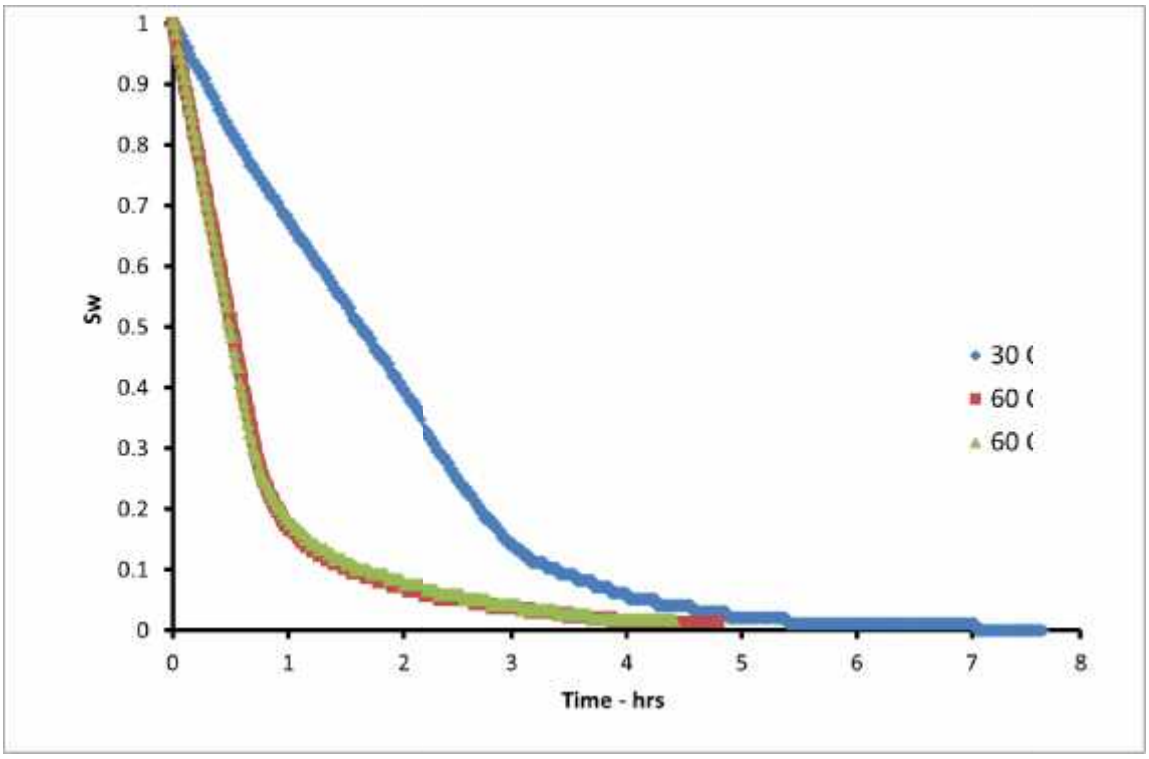

Figure 2 Effect of temperature on dry-out for water in a 2 cm Bentheimer core.

Figure 3 shows the results from dry-out experiments at 60°C in cores of two different lengths. Again, in both cases the drying rate was constant to low saturations (below 0.2) indicating that the change at low saturations is an end effect not necessarily associated with the breaking of the capillary bridge to the exposed face.

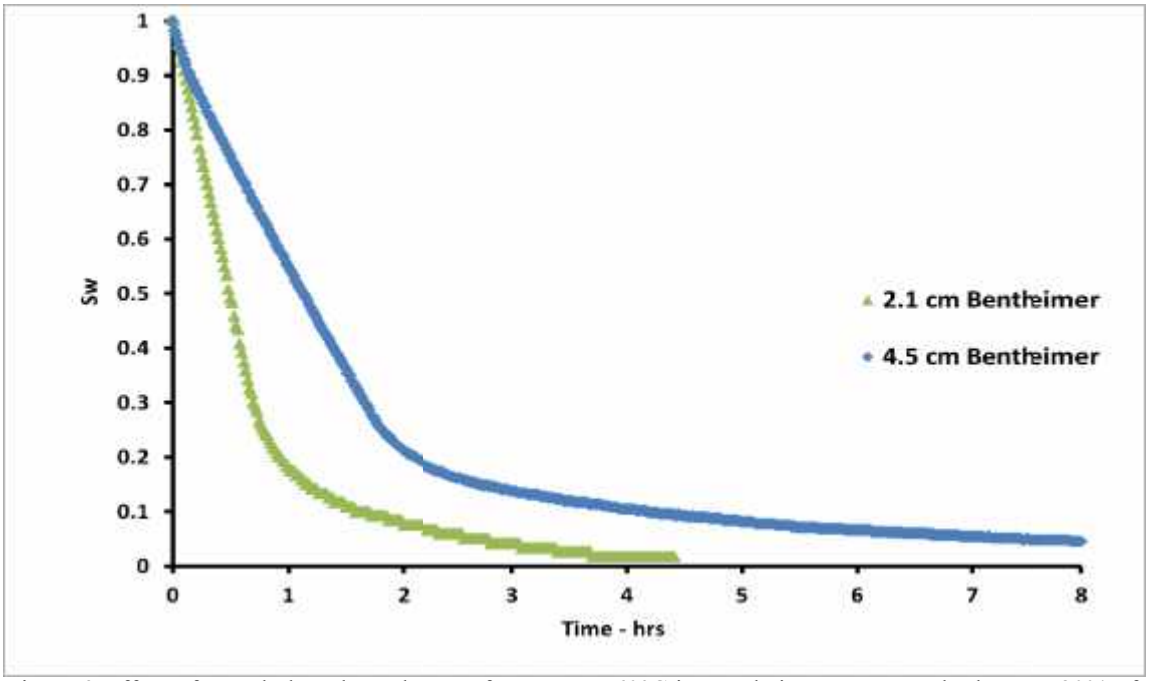

Figure 3 Effect of sample length on dry-out for water at 60°C in Bentheimer cores. In both cases 80% of the drying happens in the constant rate regime.

The final set of experiments on Bentheimer core, shown in Figure 4, explores the influence of dissolved salt (NaCl, saturated solution at ambient temperature) on the drying rate. An initial period during which the drying rate was similar to that in the earlier experiments with water (shown here for comparison) can be explained by the difference in solubility of NaCl at ambient temperature (during preparation of the saturated solution) and at the test temperature. A small amount of drying occurs before the salt starts to precipitate. Subsequently the evaporation rate slows and becomes more variable as the salt deposits grow. Interestingly, the general trend of the mass loss in this period appears to become linear with the square root of time.

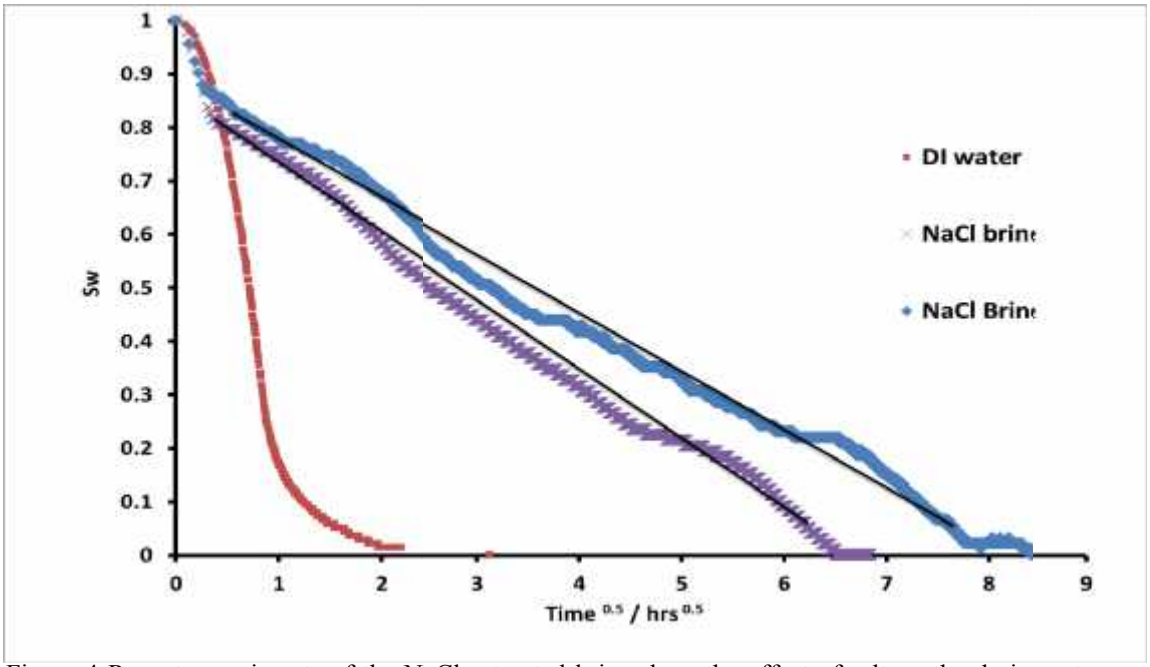

Figure 4 Repeat experiments of the NaCl saturated brine show the effect of salt on the drying rate vs. de-ionised water at 60°C on Bentheimer samples. Lines have been added to guide the eye.

The main observation from the micro-CT scanning of the sample at the end of the dry-out experiment with the saturated NaCl brine is that most of salt deposits are located in a small area just at the evaporating surface of the sample and underneath it to around one grain diameter. Figures 5 and 6 show an example Ketton limestone (as data from Bentheimer are not yet available) at the end of a 60°C dry-out with NaCl brine (saturated at ambient temperature). This is indicative of a capillary driven flow to the surface through the liquid phase causing the salt crystals to deposit only near the surface. The approximately square root time behaviour shown in the mass loss data must therefore arise from the development of the salt layer on the outer face of the sample and not from a diffusion limited process deep within the matrix of the porous media.

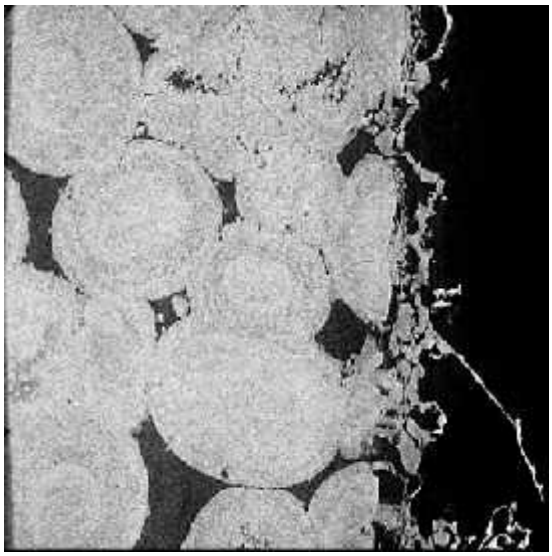

Figure 5 Micro-CT images of a Ketton sample at a 2.5 μm pixel size with field of view 2.5 mm. Salt deposition can be seen at the surface and to approximately one grain diameter into the core.

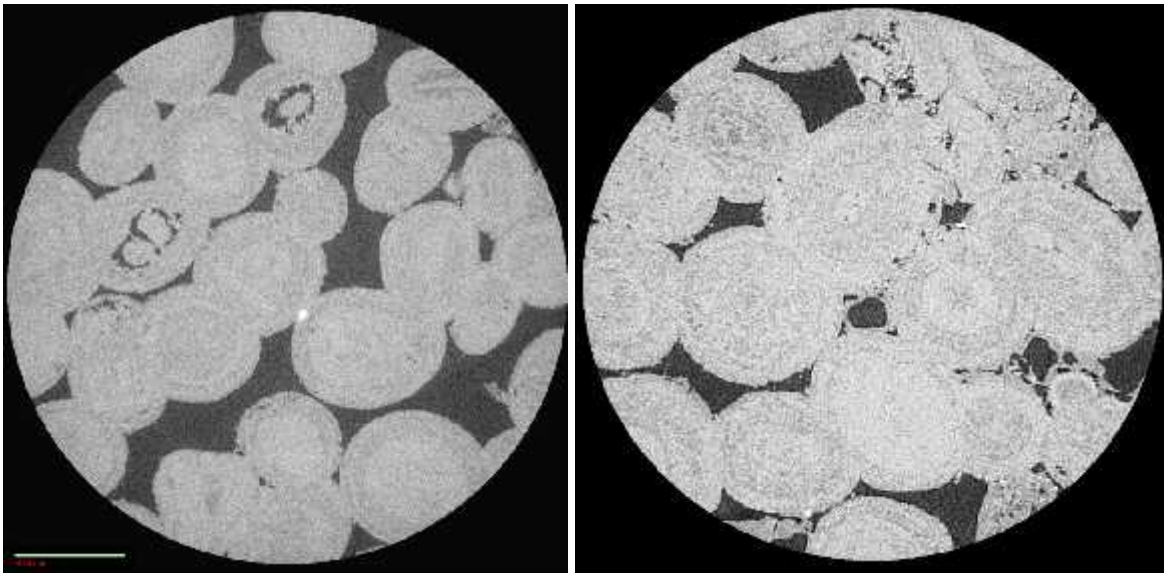

Figure 6 A 2.5 µm pixel size with field of view 2.5 mm images of a Ketton sample were taken after complete dried out. Salt deposition can be seen in the slice on the right taken at a depth of 0.5 mm from the surface but not in the image on the left take from a depth of 4 mm form the exposed surface.

CONCLUSION AND FUTURE WORK

Dry out experiments of different solutions were carried out on cores with one face exposed to represent a fractured system. In experiments with water filling the pore space, the mass loss during drying was linear in time showing that a continuous connection through the liquid phase was maintained throughout most of the process in cores up to 4.5 cm in length. In experiments with saturated NaCl brine, most of the salt was precipitated near the evaporating surface, again indicating a capillary driven flow of liquid to the surface where all the evaporation took place. However in these brine experiments the mass loss was approximately linear in square root time.

The deposition of salt at the exposed fracture face driven by capillary flow of the liquid phase in the porous matrix could cause a seal to develop and alter the storage capacity of an aquifer. A numerical model will be used in future work to calculate the permeability reduction in our samples due to salt precipitation and compare the predictions to experimental measurements on the salt deposits [8].

ACKNOWLEDGMENTS

We would like to thank our sponsors Qatar Petroleum, Shell and the Qatar Science & Technology Park for funding our project within Qatar Carbonates and Carbon Storage Research Centre, QCCSRC.
We also thank Holger Ott for the valuable discussion on dry-out.

REFERENCES

1. Peysson, Y., Bazin, B., Magnier, C., Kohler, E., and Youssef, S., “Permeability alteration due to salt precipitation driven by drying in the context of CO2 injection” Energy Procedia, (2011), 4: 4387-4394.

2. Ott, H., de Kloe, K., Marcelis, F., and Makurat, A., “Injection of supercritical CO2 in brine saturated sandstone: Pattern formation during salt precipitation” Energy Procedia, (2011), Volume 4, Pages 4425–4432

3. Bacci G, Korre, A., Durucan, S., “Experimental investigation into salt precipitation during CO2 injection in saline aquifers” Proc. 10th Int. Conf. Greenhouse gas technologies, (2011), 19-23 September, Amsterdam Energy Procedia.

4. Shokri, N., and Or, D., “What determines drying rates at the onset of diffusion controlled stage-2 evaporation from porous media?”, Water Resour. Res., (2011), 47, W09513.

5. Chauvet, F., Duru, P., Geoffroy, S., Prat, M., “Three Periods of Drying of a Single Square Capillary Tube”, Physical Review Letters, (2009), 103.124502

6. Scherer, G. W., “Theory of drying”, J. Am. Ceram. Soc., (1990), 73, 3–14.

7. Chauvet, F., Duru, P., & Prat, M., “Depinning of evaporating liquid films in square capillary tubes: Influence of corners’ roundedness”, Physics of Fluids. (2010), 1.3503925

8. Yang, J., Boek, E.S., “A comparison study of multi-component Lattice Boltzmann models for flow in porous media applications”, Computers & Mathematics with Applications, Volume 65, Issue 6, March 2013, Pages 882-890, ISSN 0898-1221